scientific reports

Check for updates

OPEN

Roadway roof stability grading method based on multi-index optimization

Xiaoqiang Xue[1], Wei Du[1], Jian Cui[2] & Wenxing Zhang[3]✉

Currently, most of the roadways adopt one support design strategy, which leads to high stress and insufficient support parameters in some crushed areas of the roadways and excess support parameters in some stable regions. There is an urgent need for a reliable method of grading the roadway perimeter rock to realize a reasonable support design for the whole area and cycle of the roadways. Taking Xiaobaodang No.1 coal mine as the background, Based on previous research, we utilized SPSS to analyze the data and selected ten indicators that significantly influence roof stability and are easily obtainable. The relatIVe weights between the influencing factors were determined using the hierarchical analysis method. The results showed that fIVe key factors, namely, roadway depth, roof strength, direct roof thickness, mining height, and rock integrity, emphatically affect the roof's stability. Based on the borehole data in the study area of the mine, 40 sets of borehole data were processed using normalization, and based on the weights of the influencing factors, a classification formula for the stability of the roadway perimeter rock was proposed to classify the boreholes initially. The roadway roof stability classification model of the BP neural network is constructed. The accuracy of the training set of 40 sets of drill hole data is 92.8%, and the accuracy of the test set is 91.7%. The classification results of the model are verified by using the mine pressure data of the mined face, and the mine pressure data shows a noticeable step change with the classification results, which puts forward theoretical references for the subsequent differentiated support of the working face. Numerical simulation software is used to analyze the vertical stress of different types of roof layers and the vertical stress of coal pillars, and the vertical stress of coal pillars at the roof layers that are highly prone to collapse of the roof is higher than that at other roof layers, so it is necessary to strengthen the support.

Keywords Enclosure stability classification, Hierarchical analysis method, BP neural network, Borehole data, Numerical simulation, Coal mine safety

China's coal mines dig new roadways up to 12,000 km[1,2] every year, and the stability and reliability of the roadway perimeter rock and scientific and reasonable control are still the focus and difficulty of scholars' research at home and abroad. However, the existing roadway support parameters are primarily designed using the engineering analogy method. The support parameter design lacks basis and is not targeted, and most of the mines use one kind of support parameter for the whole roadway; therefore, there is an urgent need for a classification method that can truly reflect the stability of the roof plate of the roadway, and provide a scientific basis for the support of the roadway[3,4].

Phase One: Before 1970, During this period, rock mass quality classification was predominantly based on single-factor methods; Key approaches included. Protodyakonov proposed the Protodyakonov coefficient classification method from the former Soviet Union. The uniaxial compressIVe strength classification method for rocks was introduced by Savarenskiy, who was also from the former Soviet Union. The classification method proposed by Terzaghi combined rock-type descriptions with rock load. Lauer's classification method was proposed by Lauer from Austria. Deere from the United States introduced the Rock Quality Designation (RQD) classification method.

Phase Two: From the 1970s to the Present. Rock mass quality classification methods have evolved from single-factor to multi-factor approaches. These methods integrate multiple factors to assess rock mass quality and link the evaluation results to practical engineering applications, forming a comprehensIVe rock mass quality

[1]Shaanxi Xiaobaodang Mining Co., Ltd., Yulin 719000, China. [2]Department of Emergency Management of Shaanxi Province, Xi'an 710018, China. [3]College of Energy and Mining Engineering, Xi'an University of Science and Technology, Xi'an 710054, China. ✉email: 18192301851@163.com

classification system. As rock mass quality classification serves as a critical basis for excavation support and long-term stability maintenance of surrounding rock in tunnels, it has garnered increasing attention from researchers and has been studied more extensIVely.

Currently, mainstream rock mass classification methods, both domestically and internationally, are predominantly based on multi-factor influence indicators, utilizing machine learning networks to classify surrounding rock data. Li Yingfu[5] classified the mining roadway according to the lithology of the surrounding rock in the influence circle of the roadway, joints and fissures, and roadway drenching, etc., and classified the stability of the roadway roof, floor, coal gangs, and coal columns of the roadway by using the slope change of the plasticity rate of the surrounding rock; finally, differentiated support was provided for the surrounding rock according to the service life of the roadway, the type of the area, the overall classification, and the sub-classification of the surrounding rock. Michael Melville[6] studied the information of logging data through the BP neural network and finally drew the geotechnical engineering hazard map to guide the production of working face; Ren[7] et al. established a BP neural network prediction model to classify the stability of the anchor rods through six evaluation indexes. Support coal mine stability classification through six evaluation indexes, using surfer software to draw the contour map of roof stability; Bai, Guangxing[8] Based on the theory of man, machine, environment, and pipe system, with the four single elements and the whole system of a coal mine as the object of research, a systematic analysis and research on the evaluation and continuous improvement of the intrinsic safety of coal mines are carried out. A BP neural network evaluation model is utilized to analyze and research the inherent safety of coal mines.

Certain scholars have classified specific mine roadways by leveraging the stress distribution patterns of surrounding rock, employing theoretical analysis, numerical simulations, and other methodologies. Cheng Lixing[9] et al., for the isolated island face of a kilometer-deep shaft, analyzed the stress of roadway peripheral rock, the stress of the roadway peripheral rock, and the stress of the roadway peripheral rock. By examining the stress evolution characteristics of the roadway perimeter rock, the roadway in front of the working face is dIVided into four types of areas according to the degree of influence of mining and puts forward the roadway support countermeasures; Hua Xin Zhu[10] For the contraction degree of the roadway section along the empty roadway after mining, dIVides the roadway section into 3 degrees of management areas, and puts forward the "perimeter rock structure zoning actIVe and passIVe support" technology; Jian Wei Zheng analyzes different kinds of support areas, and puts forward the "perimeter rock structure zoning actIVe and passIVe support" technology. Zheng Jianwei[11] studied the response characteristics of the surrounding rock under different lateral stress coefficients and obtained the key support objects for the surrounding rock of the roadway under matlab surfer different lateral stress conditions; Jiang Lishuai[12] et al. classified the overlying rock layers into seven categories by studying the structure of the rock layer overlying the roadway, the deformation and damage characteristics of the roadway roof and the equilibrium structure, and set up a graded support scheme for the roof; Malkowski, P[13]. Integrated geological, geomechanical, and mining data to propose two indices, the Roadway Design Efficiency (RDE) and the Roadway Functionality Maintenance (RFM), for rapid assessment of surrounding rock stability and compared them with on-site measurement results.

In the actual production of mines, fast and accurate roadway classification methods are essential to ensure the stability of the surrounding rock[14–16]. This paper refines and optimizes classification indicators through research on integrating multi-factor comprehensIVe evaluation and machine learning, drawing on the principles of systematic analysis to address issues in existing research, such as difficulties in obtaining indicators and limited application scenarios. A high-precision and unIVersally applicable roadway classification method is proposed, achieving rapid and rational zoning of roadways. Based on the above analysis, the process is applied to classify the surrounding rock of roadways in panels 11 and 13 of Xiaobaodang No. 1 Coal Mine. This method can also provide a theoretical foundation for roadway zoning support in other mines.

Project overview

The geological and tectonic type of Xiaobaodang No.1 coal mine is simple, the kind of stability degree of the 2–2 coal seam is simple, the type of gas is simple, the sort of hydrogeology is medium, the type of roof of the coal seam is simple, and the kind of coal mine geology is medium. The 2–2 coal of Xiaobaodang No.1 Coal Mine is the thickest central mineable coal seam in the mine, with a mineable area of 97.401 km^2, which is mineable in the whole region, and the thickness of the 2–2 coal is 3.04–9.86 m, with an average coal thickness of 5.37 m.

The depth of the 2–2 coal seam is 199.69–401.22 m, and the elevation of the bottom plate of the coal seam is 1015–890 m. The bare roof of 2–2 coal seam is medium-grained sandstone and locally coarse-grained sandstone, with a thickness of 18.92–25.9 m, an average thickness of 22.41 m, and the saturated compressIVe strength of the bare roof ranging from 16.2 to 27.2 MPa, an average of 21.6 MPa.The direct roof of the seam has the lithology of powder sandstone, with a thickness of 1.041–1.85 m, average thickness of 1.45 m, saturated compressIVe strength of direct roof 17.2- 25.3 MPa, average of 21.3 MPa.

The bottom plate of the coal seam is dominated by sandy mudstone and siltstone, with a rock thickness of 2.96–7.42 m and an average thickness of 5.19 m. The saturated compressIVe strength of the rock ranges from 17.1 to 25.3 MPa, with an average of 22.1 MPa. The allowable uniaxial compressIVe strength ranges from 12.8 to 18.9 MPa, with an average of 16.5 MPa, and it belongs to a softer (IIIa) bottom plate.

Xiao Bao Dang No.1 Coal Mine 2–2 coal seam is dIVided into an 11-pan area, 12-pan area, 13-pan area, and 14-pan area; at present, the 11-pan area is being mined back to 112,206 workings, succeeded by 112,206 workings, and the rest of the workings have been mined back in full; after the end of the 11-pan area mining, the plan is to carry out the mining back to the 13-pan area. The study grading area of the mine is the 11-pan area and the 13-pan area, and the plan of the mining project is shown in Fig. 1.

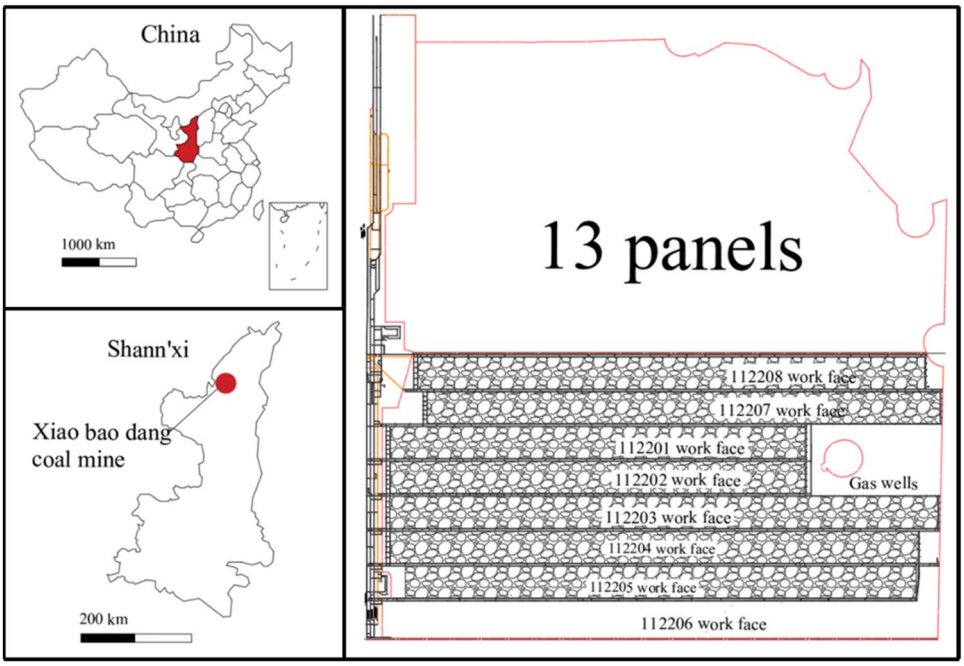

Fig. 1. Plan of the mining works in panels 11 and 13.

Number	Metric name	Number	Metric name	Number	Metric name
1	Roof Strength	2	Coal Seam Strength	3	Floor Strength
4	ImmediateRoof Thickness	5	In-Situ Stress	6	Tectonic Stress
7	Coal Roadway Burial Depth	8	Roadway Width	9	Groundwater Inflow
10	Roadway Height	11	Coal Pillar Width	12	Rock Integrity Index
13	Structural Plane Joints and Fissures	14	Initial Caving Interval of Immediate Roof	15	Mining Height
16	Ratio of Immediate Roof Thickness to Mining Height	17	Coal Seam Dip Angle	18	Rock Quality Designation (RQD)
19	Mining Method	20	Support Strength	21	Loosening Zone
22	Mining-Induced Stress	23	Angle Between Maximum Horizontal Stress and Roadway Axis	24	Initial Caving Interval of Main Roof
25	Periodic Caving Interval of Main Roof	26	Maximum Horizontal Stress	27	Coal Seam Thickness
28	Immediate Floor Thickness	29	Service Life	30	Surrounding Rock Deformation Conditions
31	Main Roof Thickness	32	Angle Between Structural Plane Strike and Roadway Axis	33	The ratio of Mining to Caving Height
34	The ratio of Mining Height to Roadway Height	35	Disturbance Conditions During Service Life	36	Influence of Adjacent Engineering ActIVities
37	Unsupported Roof Span	38	Surrounding Rock Deformation Conditions		

Table 1. Classification indicators summary Table.

Determination of the stability index of the tunnel perimeter rock

Influencing factors of roadway surrounding rock stability

Liu Chang[19] conducted a comprehensIVe statistical analysis of 38 classification indicators from 34 literature sources on coal roadway classification, based on existing research findings, using SPSS frequency analysis technology. The summary table of classification indicators is presented in Table 1, and the analysis results are shown in Fig. 2. The higher the effectIVe percentage of an indicator, the greater its recognition and acceptance in the field.

In selecting research indicators, this paper is primarily based on the following three principles: first, the indicator has a relatIVely high effectIVe percentage, reflecting its importance in practical engineering; second, the indicator data is easily accessible, facilitating practical application and promotion; and third, the redundancy among indicators is low, avoiding information overlap. However, although the effectIVe percentage of service life is relatIVely low, its impact on roof stability is of significant representatIVeness and practical importance. Over time, roof materials experience aging, leading to a decline in strength. Additionally, prolonged exposure to complex environments may result in environmental erosion, fatigue effects, and other factors, gradually reducing

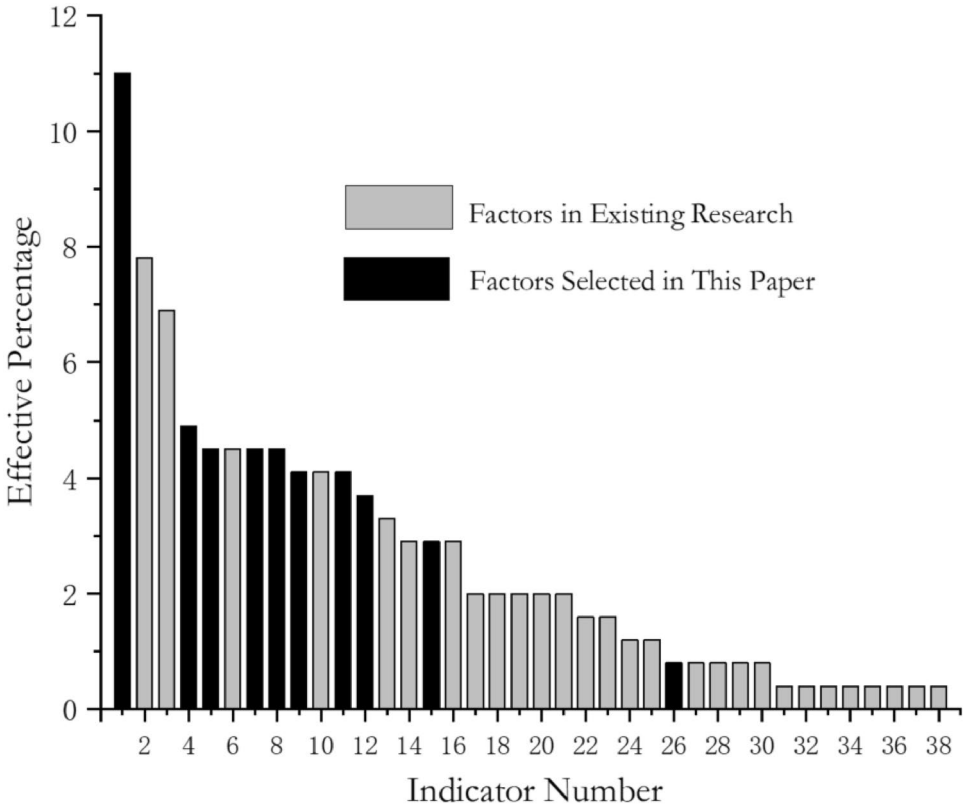

Fig. 2. SPSS frequency analysis results—histogram.

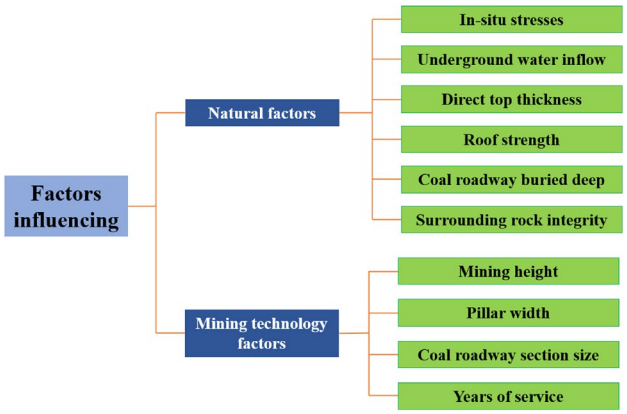

Fig. 3. Influencing factors of enclosing rock stability.

their load-bearing capacity and stability. Therefore, service life is included as one of the research indicators. The ten indicators affecting roof stability are shown in Fig. 3.

Selection of initial classification indexes for roof stability

(1) In the judgment matrices, the ratio of the importance of element i to element j is, Then the ratio of element j to element is. Therefore, there is no representation in each matrix.

Establishment of judgment matrix: The opinions of several experts were solicited, and relatIVe consistency was finally obtained after feedback and summarization of the data. The judgment matrix of the factor layer relatIVe to the indicator layer is shown in Table 2.

(2) Judgment matrix one-time test and hierarchical single sorting: judgment matrix is often a two-by-two comparison of the values obtained, so there is inevitably inconsistency. Using the consistency index and consistency ratio < 0.1 and the random consistency index of the numerical table, the judgment of the evidence is tested.

	A_1	A_2	A_3	A_4	A_5	A_6	A_7	A_8	A_9	A_{10}
A_1	1									
A_2	3	1								
A_3	4	2	1							
A_4	1/2	1/3	1/7	1						
A_5	1	1/2	1/5	1/3	1					
A_6	1/3	1/5	1/9	1/7	1/5	1				
A_7	1/4	1/3	1/7	1/7	1/7	1/2	1			
A_8	2	1/2	1/2	1/2	2	3	3	1		
A_9	2	1/2	1/2	1/2	2	3	3	1	1	
A_{10}	3	1	1	1	3	5	5	2	1	1

Table 2. Judgment matrix.

Term (in a mathematical formula)	Eigenvector (math.)	Weighting	Maximum eigenvalue	CI value
Geostress	0.649	6.492%	11.122	0.125
Roof strength	1.428	14.276%		
Roadway Depth	2.353	23.532%		
Perimeter rock integrity	1.167	11.667%		
Coal pillar width	0.675	6.755%		
Length of service	0.254	2.539%		
Underground water influx	0.237	2.374%		
Dimensions of the roadway section	0.836	8.360%		
Direct Roof Thickness	1.034	10.342%		
Mining Height	1.366	13.663%		

Table 3. Hierarchical single ordering and consistency test results.

Maximum characteristic root	CI value	RI value	CR value	Consistency test results
11.122	0.125	1.490	0.084	Pass (a bill or inspection etc.)

Table 4. Summary of consistency test results.

If the consistency test passes, the normalized feature eigenvector is used as the ranking weight.

The following formula is the consistency test index: n is the only non-zero characteristic root, is the most significant characteristic root; if I_C=0, then the judgment matrix has complete consistency, I_C the closer to 0, the greater the consistency of the judgment matrix, I_C the more significant the inconsistency, the more serious.

$$I_C = \frac{\lambda - n}{n - 1}$$

To measure the size of the value of the consistency test indicator IC, stochastic consistency test indicators, IR, are introduced. These indicators are related to the order of the judgment matrix only.

$$R_C = \frac{I_C}{I_R}$$

It is generally considered. RC < 0.1. When the judgment matrix can pass the consistency test, the test results and eigenvectors are shown in Table 3.

(3) Hierarchical total sorting: Calculate the weight of the factor layer relatIVe to each indicator layer for the hierarchical total sorting; first of all, consistency test, consistency ratio Rct for the following formula, if Rct 0.1, that the hierarchical total sorting can be through the consistency test. As shown in Table 4.

$$R_{ct} = \frac{a_1 I_{c1} + a_2 I_{C2} + \cdots + a_m I_{cm}}{I_R(a_1 + a_2 + \cdots + a_m)}$$

In the above equation, a_1 and a_2 am are the weights of m elements in the indicator layer relatIVe to the target layer. Icj is the consistency test index of the A_j judgment matrix in the factor layer to the indicator layer. After calculation, it can be obtained that CR = 0.084, passing the consistency test.

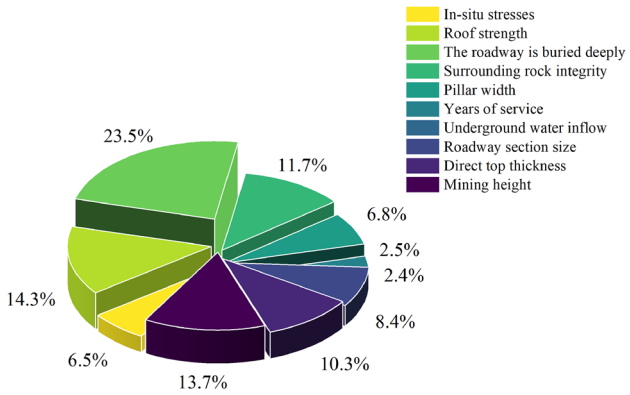

Fig. 4. RelatIVe weights of top plate classification indicators.

criterion	Indicator layer	Retrieve a value	RelatIVe weight	PositIVe and negatIVe
Geological factor	Overburden Depth	Roadway depth/m	32.03%	Turn one's back on
	Roof strength	Take the uniaxial compressIVe strength of each rock layer within 1.5 times the lane's width. The weighted average is the strength of the roof perimeter rock/MPa	19.43%	Greater than zero
	Direct roof Thickness	Thickness of direct roof of coal seam/m	18.60%	Greater than zero
	Surrounding rock integrity	Take the periodic weighting interval at the borehole-adjacent working Face /m	14.06%	Turn one's back on
Engineering factors	Mining Height	Coal mining height/m	15.88%	Turn one's back on

Table 5. Top plate classification index value.

(4) Evaluation model analysis: As can be seen from Fig. 4, the relatIVe weights of the factors affecting the stability of the roadway roof are, in descending order, the depth of the roadway, the strength of the roof, the mining height, the integrity of the surrounding rock, the thickness of the direct roof, the service life, the amount of water influx, and the index of the stress, and the relatIVe weights of the factors affecting the roof of the roadway are 10% or more, and it is determined to take the depth of the roadway, the strength of the roof, the mining height, the integrity of the surrounding rock, and the direct roof thickness as the discriminating index. Roof thickness as discriminatIVe indexes.

Optimizing the classification indicator system

By analyzing the many influencing factors of roof stability, the roadway depth, surrounding rock strength, direct roof thickness, mining height, and rock integrity, which have more relatIVe weights of each index, are selected as the indexes to categorize the roadway's roof stability. Based on the weights obtained by the hierarchical analysis method, the relatIVe weights between the fIVe selected indicators are determined, as shown in Table 5.

Data set construction

According to the basic information, such as the drill hole data of Xiaobaodang coal mine, based on the indexes obtained after screening and the method of taking values, the index value of each drill hole is obtained and summarized as the original data. According to the index parameters of the roadway perimeter rock roof, the stability level of each drill hole is categorized. However, due to the different scale between the indicators and the degree of change in the value considerable, it must be standardized, that is, the original data for the dimensionless processing; this paper selects the standardization of the extreme difference processing, the formula is shown below:

$$X'_{ij} = \frac{X_{ij} - \min_j X_{ij}}{\max_j X_{ij} - \min_j X_{ij}} \qquad PositIVe\ Indicators$$

$$X'_{ij} = \frac{\max_j X_{ij} - X_{ij}}{\max_j X_{ij} - \min_j X_{ij}} \qquad \text{negative } Indicators$$

Where [?] denotes the j observation for the I indicator.

The data for the standardized processed metrics all take the value of [0,1] and are dimensionless. All metrics are transformed to positIVe.

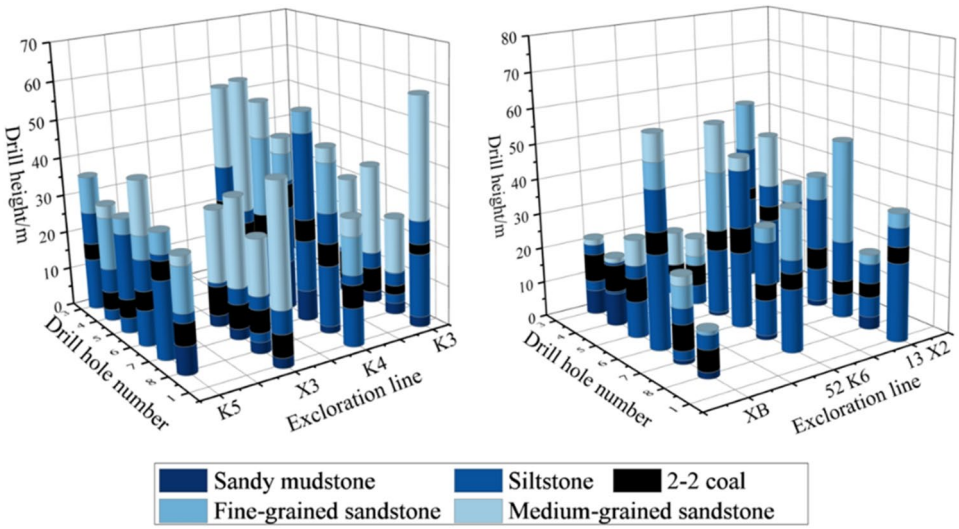

Fig. 5. Histogram of drill holes in the study area.

Term (in a mathematical formula)	Borehole number	Overburden Depth X1	Roof strength X2	Immediate roof thickness X3	Mining height X4	Perimeter rock integrity X5	Typology
1	X3-1	0.10	0.35	0.06	0.06	0.53	I
2	X3-2	0.31	0.55	0.26	0.26	0.19	II
3	X3-3	0.79	0.82	0.68	0.81	0.78	IV
4	P77	0.60	0.24	0.50	0.50	0.37	II
5	K3-5	0.43	0.68	0.11	0.11	0.37	II
6	P87	0.74	0.64	0.52	0.52	0.88	III
……	……	……	……	……	……	……	……
39	53 – 1	0.12	0.76	0.23	0.32	0.48	II
40	53 – 3	0.25	0.43	0.01	0.12	0.34	I

Table 6. Results of dimensionless quantification of indicators for standardized classifications(excerpt).

The top plate of Xiaobodang 2–2 coal seam is dIVided into 40 evaluation units according to the location of the drill holes. The order is 1, 2, 3, 4, …… and 40. The top plate is dIVided into four classes: Class I stable top plate, Class II medium stable top plate, Class III easy-to-collapse top plate, and Class IV very easy-to-collapse top plate.

The 40 sets of research area drilling column charts are shown in Fig. 5. The data of each factor of the borehole take the value of [0,1], and the relatIVe weight of each factor can be obtained by the hierarchical analysis method; for this reason, we can get the formula for the classification of the top plate grade as follows:

$$F{=}X_{1j} \times 0.32 + X_{2j} \times 0.19 + X_{3j} \times 0.19 + X_{4j} \times 0.14 + X_{5j} \times 0.16$$

$$w = x_{1j} + x_{2j} + x_{3j} + x_{4j} + x_{5j} = 1$$

The value of F in [0,0.25] is class I stabilize the top plate, in [0.25,0.5] class II medium stable top plate, in [0.5,0.75] class III easy to collapse the roof, and the value of F in [0.75,1] class IV extremely prone to collapse of the roof. Table 6 shows the dimensionless data and classification results of each classification index.

BP neural network model construction

The neural network method is a pattern recognition method without pattern recognition, characterized by adaptIVe learning ability, good at limited sample data, extracting the statistical laws, large-scale parallel processing of information, and fast operation speed.BP neural network is a typical type of multi-layer feed-forward network that adds several implicit layers between the input layer and the output layer to achieve, mainly in function approximation, classification prediction, data compression, Pattern recognition, and other fields are widely used, neural network models are realized using networks and their variations. Among them, the most commonly used is a three-layer neural network, i.e., a feed-forward network with only one hidden layer[17–19].

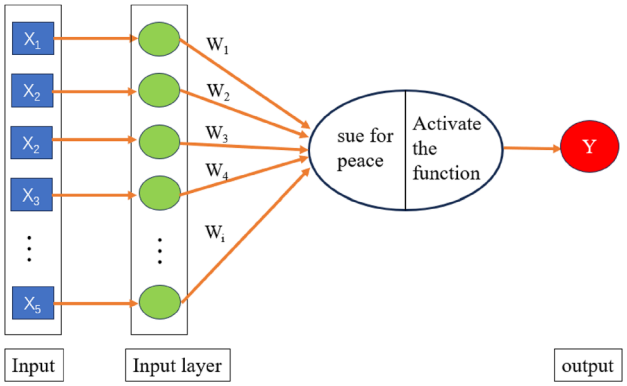

Fig. 6. Neural network training process.

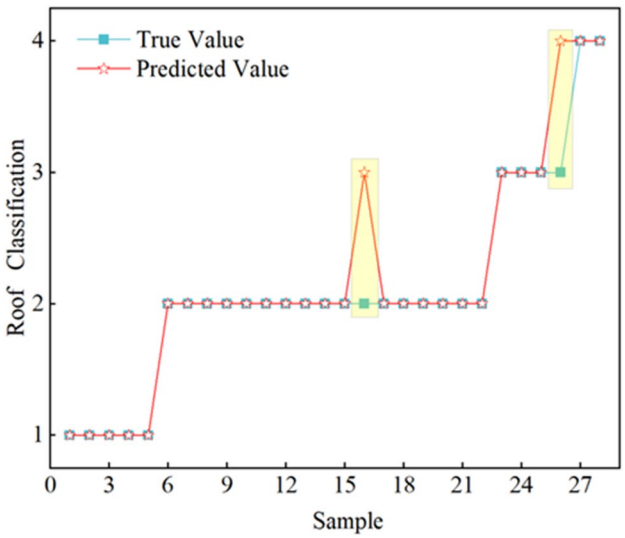

Fig. 7. Training set prediction results.

Model training and testing

There are 40 sets of data in this learning task. DIVided according to a 7:3 ratio, 28 data sets were allocated as training sets to train the neural network and optimize its internal parameters. The remaining 12 data sets were dIVided into a test set to evaluate the model's generalization ability and ensure its performance on new data.

MATLAB R2019B software was used to construct the roadway roof stability classification model based on the BP neural network, and 40 groups of drill hole sample data were analyzed in depth. The first 28 groups of drill hole roof samples that have been classified are selected as the basic data set for training the neural network. According to the hierarchical analysis method, fIVe indicators with large relatIVe weights were obtained as input vectors of the model: roadway burial depth, roof strength, direct roof thickness, mining height, and Perimeter rock integrity. As shown in Fig. 3, these indicators constitute the fIVe-dimensional input vector of the neural network. Accordingly, the input layer has fIVe neurons, each corresponding to one input index. For the output layer, the stability of the roadway roof is refined into four classes according to its stability: class I stable roof, class II moderately stable roof, class III easily collapsible roof, and class IV very easily collapsible roof. Therefore, the output layer is configured with four neurons, each corresponding to a stability class, for accurate classification prediction.

The model's output neuron is 4. Through multiple trainings, it is found that the training effect is best when the hidden layer is 6. The model training process and results are shown in Fig. 6. After training; the network means square error me is less than the 0.001 requirements, and the training effect is better.

The BP neural network is utilized to train the first 28 sets of samples, and the training results are shown in Fig. 7, and the latter 12 sets of samples are tested. The test results are shown in Fig. 8. As can be seen from Fig. 7, the prediction results of the training set match with the actual, and the accuracy rate reaches 92.8%, in which all the predictions of the first-class stabilized top plate and the fourth-class top plate are correct, and the third-class stabilized top plate and the second-class medium stabilized top plate each have a group of samples with wrong

predictions. It indicates that using the data around the mined and excavated roadways as the training set, the grading results are accurate and reliable and provide reference value for the test set.

As can be seen in Fig. 8, the test set's prediction results match the true values with an accuracy of 91.7%. Eleven out of the 12 data sets are correctly predicted, and only one data set is incorrectly predicted.

Analysis and evaluation of results

The data in Table 6 were generated based on the plan view of the mining project using Surfer 17 software. The top plate classification results of 40 sets of drill hole data are shown in the following figure, in which the red drill holes are the distribution of the training set, and the blue drill holes are the distribution of the test set.

As can be seen from the figure, the roof plate classification is dominated by stable peripheral rock roadway and medium stable peripheral rock roadway, and the medium stable peripheral rock accounts for the most significant proportion, the part of each working face near the stoping line in the 11 cross-sectional area is easy to collapse roof plate and very easy to collapse roof plate, when the working face is mined back to this area, it is necessary to carry out monitoring of the mining pressure, strengthen the roof plate support parameters, and prevent the roof phenomenon in the roadway, the 11 cross-sectional area 112201,112202, 112,203, 112,204 synthesized mining face cut in front of the range of 900–1800 m is easy to collapse perimeter rock roadway. 13 plate area compared to the 11 plate area roadway perimeter rock is more stable, stable roof and medium stable roof perimeter rock roadway accounted for a more significant proportion, easy to collapse roof accounted for a smaller proportion, when mining back to this area, need to strengthen the mine pressure monitoring, very easy to collapse roof accounted for a small proportion. The proportion of highly vulnerable roof layers is tiny. Table 6 was generated using the surfer 17 software, and the 2–2 coal section grading diagram is shown in Fig. 9.

Engineering validation

Validation of the roof hazard classification is essential to ensure its accuracy and reliability. In addition, grading validation allows us to test whether the model meets our expectations, such as whether it can accurately categorize data or predict outcomes. By performing model validation, we can better understand the model's limitations and take steps to improve its performance before applying it to real-world problems. Thus, model validation is essential to ensure the usability and reliability of a model.

For the roadway, the more complex the roof plate is, the more stable it is, and for the working face, the more complicated the plate will inevitably lead to an increase in the distance of the roof plate's periodic collapse. Then, the periodic pressure will result in enormous pressure on the roof plate. We now dIVide the roof plate into stabilized top plate, medium stable top plate, easy to collapse the roof, and highly prone to collapse of the roof; for the working face coal pressure, stabilized the top plate working face coal pressure shows the more intense, extremely prone to collapse of the roof working face coal pressure shows the weakest.

As shown in Fig. 10. The mine pressure data of the four types of roof plates are consistent with the results of roof plate dIVision, and the average value of the mine pressure data of the very easy-to-fall roof plate is the lowest, 25.6 MPa. The smaller the mine pressure data, the highly prone to collapse of the roof is; it means that the roof plate here is more and more broken, and it is necessary to regulate the parameters of the support; the average value of the mine pressure data of the stabilize the top plate is the highest, which is 33.9 MPa, indicating that the roof plate here is more and more hard and stable; the difference in the average value between the medium stable top plate area and easy to collapse the roof area is 8.3 MPa.

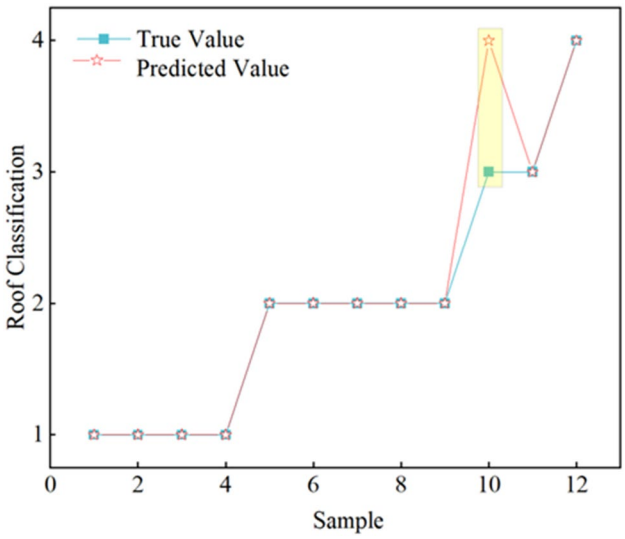

Fig. 8. Prediction results of the prediction set.

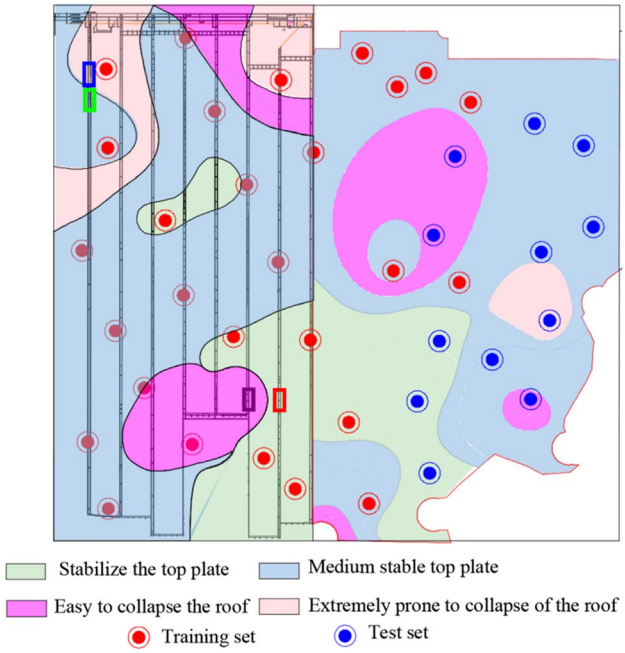

Fig. 9. Xiaobodang No. 1 coal mine enclosure rock classification map.

Numerical simulation validation

Modeling

Using FLAC3D 6.0 Numerical Simulation Software, the actual conditions of the Xiaobaodang coal mine are used as the background to build the model with the dimensions of 502 m*5 m*91 m (x*y*z). A 6.5 m*5 m*4.5 m and a 5.5 m*5 m*4.5 m roadway were excavated first, and then the 112,204 working face was excavated with a size of 350 m*5 m*7 m. The roadway perimeter rock cell was accurate to 0.5 m. A vertical load of 7.6 MPa was applied on the upper part of the model to simulate the self-weight of the overburdened rock layer, and the model was surrounded by a fixed constraint at the perimeter and bottom. As shown in Fig. 11.

According to the mechanical test results of the coal rock body provided by on-site geological investigation and related research, and considering the scale effect of the coal rock body, the physical and mechanical parameters of the coal rock body adopted for simulation calculation are shown in Table 7.

Vertical stress distribution in the top plate

(1) Vertical stress distribution on the roof plate during roadway excavation.

Figure 12 shows the vertical stress distribution of the horizontal section at different distances from the roadway roof during the roadway excavation. From Figure (a), it can be seen that at the location of the rock layer section 1 m from the roadway roof, the vertical stress difference between different levels of the roadway roof is relatIVely small, and there is only a tiny change in the location of the edge of the roadway. Vertical stress maximum roadway side 10 m position, vertical stress is 10.5 MPa; from the figure (b) can be seen: from the roadway roof 3 m rock layer cross-section position, different levels of roadway roof vertical stress difference is trim, vertical stress difference appeared in the roadway is above, the rule of change is not apparent. Figure (c) can be seen in the rock layer section position of 5 m from the roof of the roadway; the vertical stress in the rock layer section position of 5 m is a "V" type distribution of different levels of vertical stress difference in the roof of the roadway is larger, the vertical stress difference mainly occurs in the upper part of the roadway and close to the edge of the roadway, and is very easy to fall to the roof of the roadway, the vertical stress is 7.5 MPa. The vertical stress is 7.5 MPa, and the vertical stress is 7.0 MPa for the stable roof roadway, and the difference in vertical stress is slight. During the roadway excavation.

(2) Vertical stress distribution of the roof plate during the workforce mining period.

Figure 13 shows the vertical stress distribution of the horizontal section at different distances from the roadway roof during workforce mining. Figure (a) shows that in the cross-section of the rock layer at 1 m from the roadway roof, the vertical stress difference between different levels of the roadway roof is significant. The vertical stress difference mainly occurs above the coal pillar. The vertical stress of varying levels of the roof rock layer right above the coal pillar is as follows: easy to collapse the roof> medium stable top plate> stabilize the top plate> extremely prone to collapse of the roof. From Figure (b), it can be seen that the vertical stress distribution characteristics of the rock section 3 m away from the top plate of the roadway are the same as those of the rock section 1 m away from the top plate and the difference in vertical stresses mainly appears above the coal pillar. The vertical stresses of the rock layers of different grades of the top plate above the coal pillar are as follows: easy to collapse the roof> medium stable top plate> stabilize the top plate> extremely prone to collapse. From Figure (c), it can be seen that in the rock layer cross-section position of 5 m from the roadway roof, the vertical

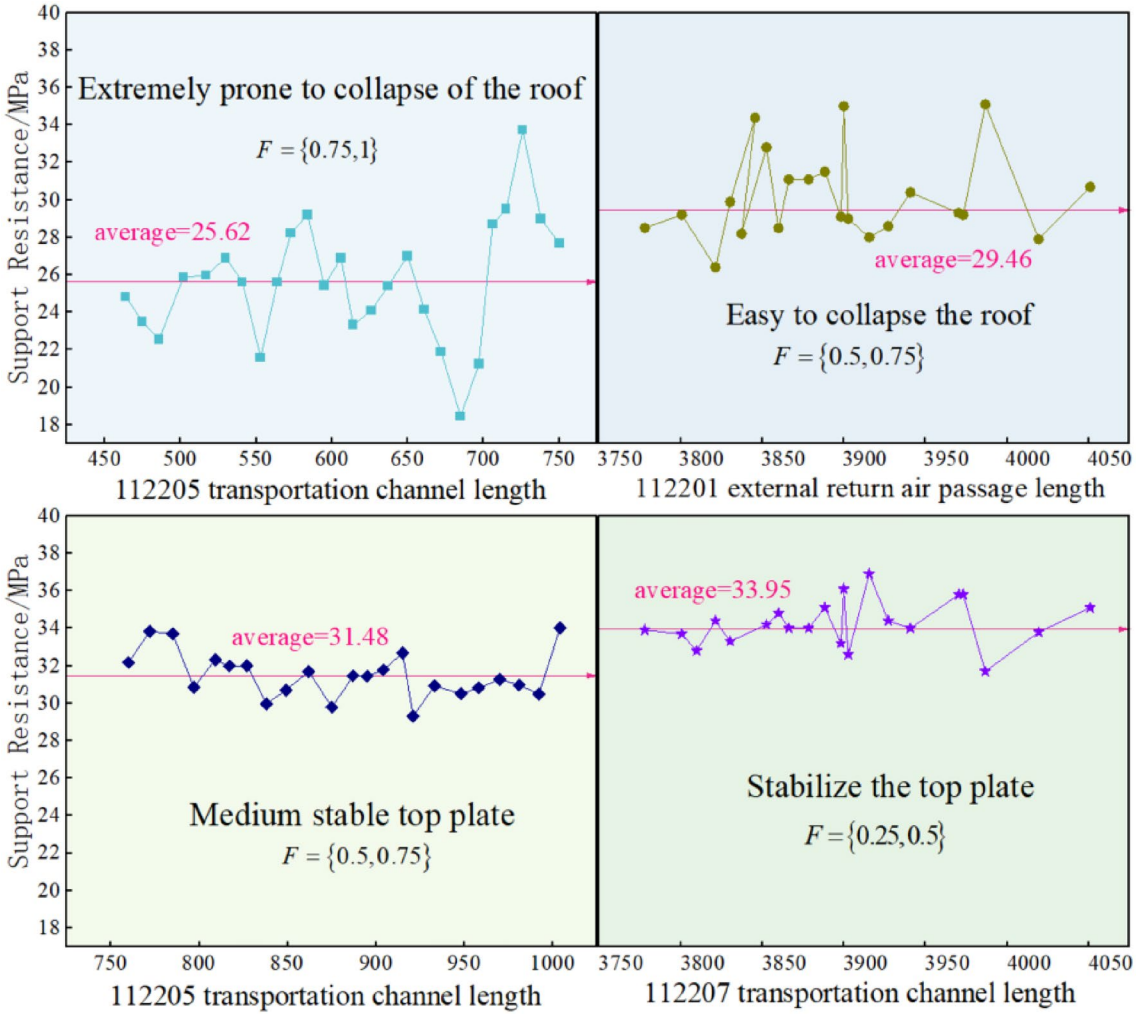

Fig. 10. Ore pressure distribution in each grading area.

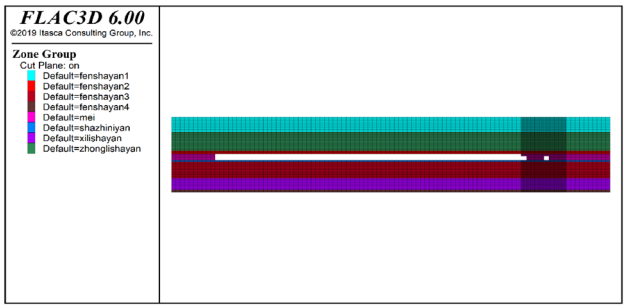

Fig. 11. Mesh diagram of FLAC3D 6.0 simulation.

stress difference of different levels of the roadway roof is more considerable; the vertical stress difference mainly appears in the position above the roadway, above the coal pillar and the edge of the working face, and the order of vertical stress of different levels of roof rock layers directly above the roadway is as follows: extremely prone to collapse of the roof> easy to collapse the roof> medium stable top plate> stabilize the top plate, the difference of vertical stress of different levels of roof rock layers directly above the roadway is 2.5 times higher than the vertical stress difference of 2.4 times higher than that of 2.6 times. The difference in vertical stress is 2.5 MPa. During mining, the vertical stress is mainly concentrated above the coal pillar, and the vertical stress in the coal pillar is 3.2 times higher than during digging. The order of vertical stresses of different levels of rock layers directly above

serial number	lithology	Density kg/m^{-3}	The angle of internal friction (°)	Cohesion /MPa	Tensile strength /MPa	Elastic Modulus /MPa	Poisson's Ratio
1	Fine-grained sandstone	2280	33	5.35	1.59	$2.96*10^4$	0.18
2	Siltstone	2560	34	1.4	1.32	$1.95*10^4$	0.21
3	Medium sandstone	2280	33	5.35	1.32	$2.4*10^4$	0.18
4	Coarse-grained sandstone	2280	35	5.04	3.48	$2.59*10^4$	0.19
6	Coal	1300	30	0.25	0.32	$0.88*10^4$	0.21
7	Sandy mudstone	2500	30	2.05	1.44	$2.7*10^4$	0.19

Table 7. Mechanical parameters of rock formation.

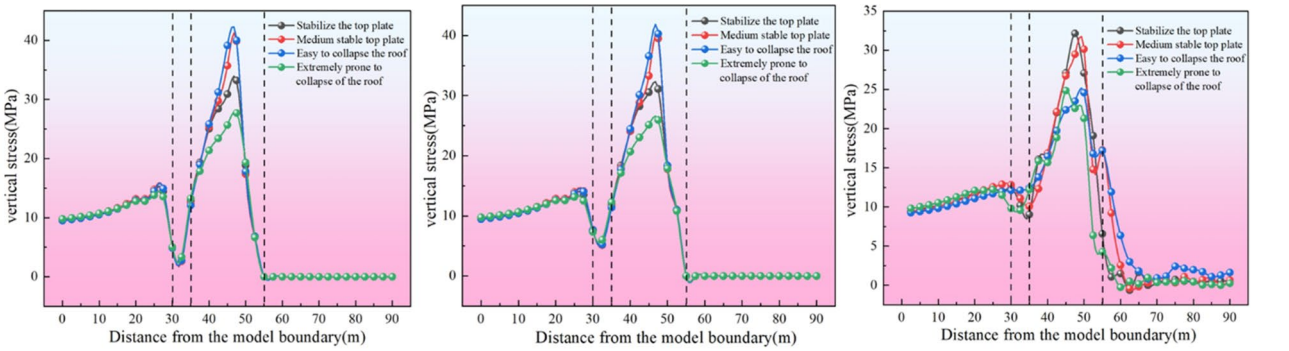

(a) 1m from the roof of the roadway (b) 3 m from the roof of the roadway (c) 5 m from the roof of the roadway

Fig. 12. Vertical stress distribution at different distances from the roof of the roadway.

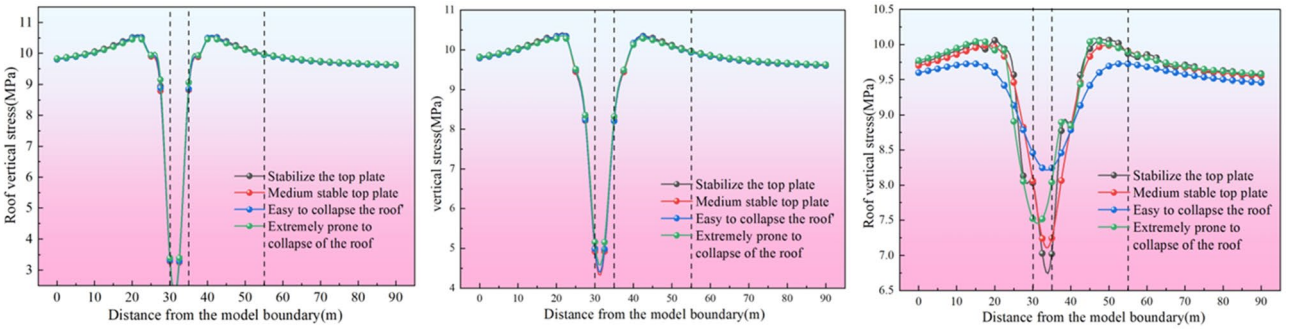

(a) 1m from the roof of the roadway (b) 3 m from the roof of the roadway (c) 5 m from the roof of the roadway

Fig. 13. Vertical stress distribution at different distances from the roof of the roadway.

the coal pillar is as follows: extremely prone to collapse of the roof< easy to collapse the roof< medium stable top plate< stabilize the top.

Vertical stress distribution in coal pillar

(1) Vertical stress distribution of coal pillar during roadway excavation.

Figure 14 shows the vertical stress distribution of the coal column during the roadway excavation. From the figure, it can be seen that during the roadway excavation, the maximum value of vertical stress is 12 MPa. The difference in vertical stress in the coal column under different levels of roof plate is minor, in which the vertical stress in the coal column under the conditions of easy to-collapse roof and highly prone to collapse of the roof plate is slightly larger than that under the conditions of stabilize the top plate and medium stable top plate, and the distribution of the vertical stress under the conditions of different levels is roughly the same. The distribution of vertical stresses under different levels is more or less the same, and the vertical stresses are small

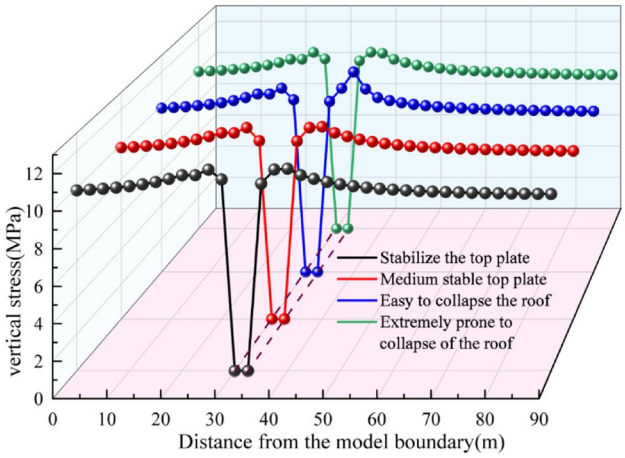

Fig. 14. Vertical stress distribution of coal pillar.

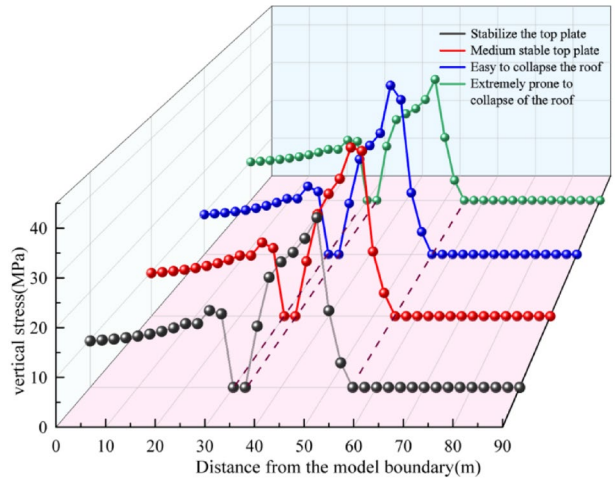

Fig. 15. Vertical stress distribution of coal pillar.

in the process of digging. The roof layers of different levels can withstand the deformation, the deformation value of the roadway is small, and the coal columns are relatIVely stable.

(2) Vertical stress distribution of the coal pillar during the face mining period.

Figure 15 shows the vertical stress distribution of the coal column during the face mining period. The figure shows that the vertical stress of the coal column under different levels of roof layers is significantly different. The vertical stress during the face mining period is significantly increased compared with that during the digging period, and the vertical stresses of varying levels of roof layers inside the coal column are as follows: easy to collapse the roof> medium stable top plate> stabilize the top plate> extremely prone to collapse of the roof. The vertical stress of the coal pillar under the easy-to-collapse roof is the largest, with a peak stress value of 40.7 MPa, and the vertical stress of the coal pillar under the highly prone collapse of the roof is the smallest, with a peak stress value of 25.9 MPa, and the difference between the two is 14.8 MPa, and the easy to collapse the roof is 1.57 times of the vertical stress of the coal pillar under the highly prone to collapse of the roof, which is because the top plate of the highly prone to collapse of the roof is more broken. By mining the long-wall working face, the surrounding rock of the coal pillar is weaker, and the coal pillar has been severely damaged. This is because the top plate is broken, the surrounding rock of the coal pillar is weaker, and the coal pillar has been seriously hurt. The vertical stress is transferred to the roadway and coal body, which results in the most minor vertical stress in the coal pillar. In the process of mining back to the top plate that is highly prone to collapse of the roof, if the roadway near the hollow area needs to continue to be used, it is necessary to strengthen the support and strengthen the observation of mine pressure to prevent the top plate from falling and other phenomena.

Conclusion

(1) Based on SPSS data analysis, This study combines the Analytic Hierarchy Process (AHP) with a BP neural network to construct a classification framework for roadway surrounding rock stability. The classification

accuracy was significantly improved, with the training and test sets achieving an accuracy rate of over 90%. A stability grade classification map for surrounding rock was developed, providing a more scientific and efficient technical approach for roadway stability evaluation.

(2) By incorporating on-site mining pressure data to validate the classification results, the study revealed a stepwise variation pattern in the mining pressure behavior of the four types of roadways. This finding provides a theoretical basis for roadway support design and mining pressure monitoring.

(3) Based on numerical simulation results, the study proposed support optimization solutions for roadways prone to roof collapse and emphasized the importance of mining pressure monitoring. These recommendations have been preliminarily applied in the Xiaobaodang Mine, significantly enhancing roadway stability and offering a practical reference for coal mines with similar geological conditions.

Discussion

The results indicate that the classification of the surrounding rock of the tunnel is consistent with the actual conditions and can serve as a theoretical basis for guiding the differentiated support of the mine. However, the limitation of the study lies in the relatIVely small sample size, which may affect the general applicability of the results. Future research could optimize the classification method and explore the stability classification of surrounding rock under different mine conditions.

Methods

This study utilized methods such as the Analytical Hierarchy Process (AHP), BP neural network, and numerical simulation to classify the roof stability of the 11-pan area and 13-pan area in Xiaobaodang No. 1 Coal Mine.

Software version description

The numerical simulations in this study were conducted using the following software tools with their respectIVe versions and developer information: MATLAB (Version R2019b, developed by MathWorks, available at https://www.mathworks.com), Surfer (Version 17, developed by Golden Software, accessible at https://www.goldensoftware.com), and FLAC3D (Version 6.0, developed by Itasca Consulting Group, obtainable at https://www.itascacg.com).

Data availability

The datasets used and analyzed during the current study are available from the corresponding author upon reasonable request.

Received: 7 January 2025; Accepted: 30 July 2025
Published online: 10 August 2025

References

1. *The Following Formatting. Styles are Meant as a Guide, as Long as the Full Citation is Complete and Clear, Frontiers Referencing Style will be Applied During Typesetting.*
2. KANG Hongpu. Support technologies for deep and complex roadways in underground coal mines: a review[J]. *Int. J. Coal Sci. Technol.* **1** (3), 261–277 (2014).
3. Hongpu, K. A. N. G. et al. Forty years development and prospects of underground coal mining and strata control technologies in China[J]. *J. Min. Strata Control Eng.* **1** (1), 013501 (2019).
4. CAI Meifeng. Keystone theory and techniques for surrounding rock stability and strata control in deep mining[J]. *J. Min. Strata Control Eng.* **2** (3), 033037 (2020).
5. Wenjun, J. U. & Yukai, F. U. Problem of roadway support in Chinese coal mines and adaptIVe strategy[J]. *Coal Min. Technol.* **20** (6), 1–5 (2015).
6. Malkowski, P. & Juszynski, D. Roof fall hazard assessment with the use of artificial neural network. *Int. J. Rock Mech. Mining Sci.* (2021).
7. Melville, M. et al. *Optimization of a Coal Mine Roof Characterization Model Using Machine Learning* (2024).
8. Ren, H. & Zhu, Y. J. Classification and application of roof stability of bolt supporting coal roadway based on BP neural network. *Adv. CIVil Eng.* (2020).
9. Gao Yongge, X. et al. Characteristics of tensile-shear rupture and zonal control method of high partial stress coal mine perimeter rock. *J. Min. Rock. Control Eng.* **6** (04), 66–79 (2024).
10. Lixing, C. H. E. N. G. et al. Characteristics of mining stress zoning evolution of tunnel perimeter rock in deep well Island working face [J]. *Geotechnics* **41** (12), 4078–4086. https://doi.org/10.16285/j.rsm.2020.0441 (2020).
11. Xinzhu, H. U. A. et al. Research on deformation mechanism and zoning management technology of perimeter rock in deep wells with cut tops. *J. Min. Saf. Eng.* **41** (04), 655–665 .https://doi.org/10.13545/j.cnki.jmse.2023.0189 (2024).
12. Jianwei, Z. et al. Characterization of differential response to tunnel deformation and analysis of support design. *J. Min. Rock. Control Eng.* **3** (03), 13–20 (2021).
13. Małkowski, P., Niedbalski, Z. & Majcherczyk, T. Roadway design efficiency indices for hard coal mines. *Acta Geodyn. Geomater.* **13** (2), 201–211 (2016).
14. Yingfu, L. I. et al. Classification of dynamic weights and their differentiated support for the back-mining roadway in the Northern Anhui mining area. *J. Min. Saf. Eng.* **34** (06),1042–1050 .https://doi.org/10.13545/j.cnki.jmse.2017.06.002 (2017).
15. Lishuai, J. I. A. N. G. et al. Characteristics of deformation and damage of composite roof slab in roadway and classification of potential risk of roofing. *J. Coal.* **39** (07), 1205–1211. https://doi.org/10.13225/j.cnki.jccs.2013.1219 (2014).
16. Bai, G. & Xu, T. Coal mine safety evaluation based on machine learning: a Bp neural network model. *Comput. Intell. Neurosci.* (2022).
17. He Manchao, W. et al. Progress in rock mechanics for deep mining [J]. *J. China Coal Soc.* **49** (01), 75–99. https://doi.org/10.13225/j.cnki.jccs.2023.1400 (2024).
18. Xie Heping, M., Hongyan, Z. & Hongwei Strategic research on the development of mining discipline in China during the fourteenth FIVe-Year plan period. *China Sci. Found.*. **35** (06), 856–863. https://doi.org/10.16262/j.cnki.1000-8217.2021.06.002 (2021).

19. Liu, C. *Classification of Surrounding Rock Stability in Coal Roadways and Software Development in Kaiping Mining Area* (China UnIVersity of Mining and Technology, 2024).
20. Xie, H. et al. Opportunities for the development of the coal industry under the carbon neutrality target. *J. China Coal Soc.* **46** (07), 2197–2211. https://doi.org/10.13225/j.cnki.jccs.2021.0973 (2021).
21. Geise, S., Emery, J. & Canbulat, I. *Assessment of Development Roadway Roof Conditions at an Operating Underground Coal Mine Using Neural Network Analysis* (2019).
22. Bressler, N. How do you check the accuracy of your machine learning model?. https://deepchecks.com/how-to-check-the-accuracy-of-your-machine-learning-model/ (Accessed 5 April 2024) (2022).

Author contributions

Supervision, X.X; Resources, X.X.; Investigation, W.D.; Data curation, W.D.;Conceptualization, J.C; Formal analysis, J.C.;Methodolog, J.C.; Writing-originaldraft, W.Z.; writing-review & editing, W.Z. All authors haveread and agreed to the published version of the manuscript.

Declarations

Competing interests

The authors declare no competing interests.

Additional information

Correspondence and requests for materials should be addressed to W.Z.

Reprints and permissions information is available at www.nature.com/reprints.

Publisher's note Springer Nature remains neutral with regard to jurisdictional claims in published maps and institutional affiliations.